Proceedings of the 10th Brazilian Congress of Thermal Sciences and Engineering -- ENCIT 2004
Braz. Soc. of Mechanical Sciences and Engineering -- ABCM, Rio de Janeiro, Brazil, Nov. 29 -- Dec. 03, 2004

Paper CIT04-0443

PREDICTION OF ^{222}Rn EXHALATION RATES FROM PHOSPHOGYPSUM BASED STACKS. PART II: PRELIMINARY NUMERICAL RESULTS

José A. Rabi
Faculdade de Engenharia Civil, Pontifícia Universidade Católica de Minas Gerais – PUC Minas, campus Poços de Caldas
Av. Padre Francis Cletus Cox, 1661, Poços de Caldas, MG, 37701-355, Brazil
jrabi@pucpcaldas.br

Abdulmajeed A. Mohamad
Department of Mechanical and Manufacturing Engineering, Faculty of Engineering, The University of Calgary
2500 University Drive NW, Calgary, Alberta, T2N 1N4, Canada
amohamad@enme.ucalgary.ca

Abstract. *The first part of this paper proposes a steady-state 2-D model for ^{222}Rn transport in phosphogypsum stacks. In this second part, the dimensionless model equations are solved numerically with the help of an existing finite-volume simulator that has been successfully used to solve heat and mass transfer problems in porous media. As a test case, a rectangular shaped stack is considered in order to verify the ability of the proposed parametric approach to account for concurrent effects on the ^{222}Rn exhalation into the local atmosphere. Air flow is supposed to be strictly buoyancy driven and the ground is assumed to be impermeable to ^{222}Rn and at a higher temperature under the stack base. Dimensionless controlling parameters are set to representative values and results are presented for Grashof number in the range $10^6 \le Gr \le 10^8$, corresponding to very small to small temperature differences between incoming air and ground underneath the stack base. For the particular set of parameters and inasmuch as Gr increases, streamlines presented basically the same pattern while internal isotherms and isoconcentration lines remained almost unchanged. Total average Sherwood number proved to be rather insensitive to Gr while total average Nusselt increased slightly with Gr.*

Keywords*. radon transport, phosphogypsum, porous media, heat-mass transfer, numerical simulation*

1. Introduction

Understanding ^{222}Rn generation and transport in porous media can be a useful tool for the analysis of environmental issues related to large-scale utilization of phosphogypsum, a by-product from the phosphate fertilizer industry. This is because radiation exposure assessment and radiological protection design are ultimately based on ^{222}Rn exhalation rates. Transport of such radioactive gas across a porous matrix involves several physical factors concurrently as for instance emanation rate, material porosity and permeability, moisture content, temperature and mass diffusivity.

As a result, a comprehensive model is likely to become quite involved and the nuclear physicist or engineer should rely on numerical simulation. Since the recognition of exposure to ^{222}Rn decay products among uranium miners in the 1950s, the scientific community's attention to radon problems has increased greatly (Nero, 1988). Nonetheless, to the authors' knowledge, numerical simulation of ^{222}Rn transport in porous media is quite recent.

Loureiro (1987) implemented a finite-difference method to predict radon entries into house basements from underneath soil gas (air). This same author later helped to improve an existing numerical simulator for ^{222}Rn transport in soil (Yu *et al.*, 1993). Andersen (2000) developed a finite-volume computational code for the same kind of problem, including transient phenomena and 3-D domains. Fluctuations in the driving pressure difference were investigated by Riley *et al.* (1999). The simulator used by Bertozzi *et al.* (2002) is intended to predict ^{222}Rn exhalation rates from phosphogypsum stacks but their initial version is designed to 1-D domains and steady-state.

More recently, an existing finite-volume computational simulator was adapted to accommodate natural convection as well as ^{222}Rn decay and possibly emanation effects inside the porous matrix (Rabi and Mohamad, 2004). In addition, governing equations numerically implemented in the computational code are written in dimensionless form in order to account for concurrent effects of controlling physical parameters.

The first part of the paper outlined a steady-state 2-D model for ^{222}Rn transport in phosphogypsum stacks, where the buoyancy-driven air flow follows Darcy-Brinkman-Boussinesq approach. Distinct sets of dimensionless variables were proposed in accordance to the external air flow condition. In this second part, one of those sets is applied to a test case. The dimensionless governing equations are numerically solved with the help of the aforesaid computational simulator so that ^{222}Rn exhalation rates into local atmospheric air from phosphogypsum stacks can be predicted.

2. Test case definition

Figure 1 shows the phosphogypsum stack investigated and the corresponding dimensionless Cartesian coordinate system. The rectangular shaped stack of aspect ratio A = L / H is regarded as a porous medium sufficiently large in the direction normal to the plane of Fig. 1, whose porosity ε and isotropic permeability K are constant.

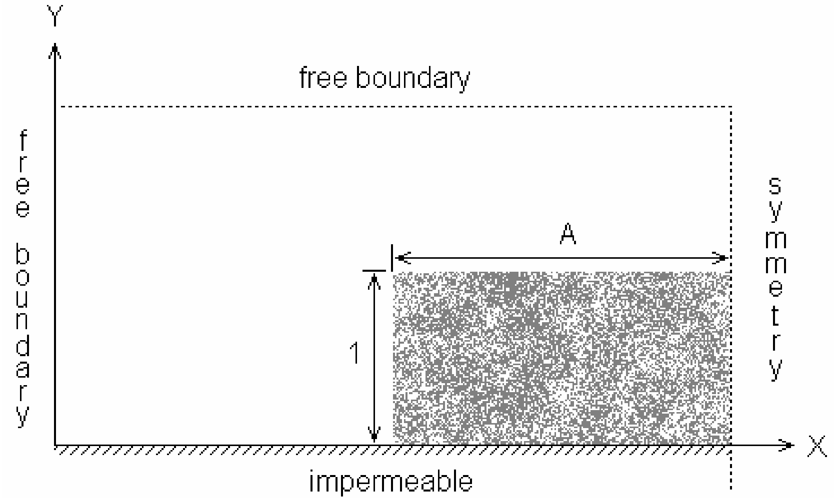

Figure 1. Schematic diagram of the rectangular shaped phosphogypsum stack investigated.

Local thermodynamic equilibrium is evoked and Boussinesq approximation is assumed for the buoyancy-driven air flow. Disregarding wind effects, it was shown in the first part of the paper that the dimensionless differential governing equations for mass, momentum, energy and species concentration are written as

$$\frac{\partial U}{\partial X} + \frac{\partial V}{\partial Y} = 0 \tag{1}$$

$$U\frac{\partial U}{\partial X} + V\frac{\partial U}{\partial Y} = \Gamma^n\left(\frac{\partial^2 U}{\partial X^2} + \frac{\partial^2 U}{\partial Y^2}\right) - \frac{\partial P}{\partial X} - n\frac{U}{\mathrm{Da}} \tag{2}$$

$$U\frac{\partial V}{\partial X} + V\frac{\partial V}{\partial Y} = \Gamma^n\left(\frac{\partial^2 V}{\partial X^2} + \frac{\partial^2 V}{\partial Y^2}\right) - \frac{\partial P}{\partial Y} - n\frac{V}{\mathrm{Da}} + \mathrm{Gr}\theta \tag{3}$$

$$U\frac{\partial \theta}{\partial X} + V\frac{\partial \theta}{\partial Y} = \frac{\Lambda^n}{\mathrm{Pr}}\left(\frac{\partial^2 \theta}{\partial X^2} + \frac{\partial^2 \theta}{\partial Y^2}\right) \tag{4}$$

$$U\frac{\partial \phi}{\partial X} + V\frac{\partial \phi}{\partial Y} = \frac{\Psi^n}{\mathrm{Sc}}\left(\frac{\partial^2 \phi}{\partial X^2} + \frac{\partial^2 \phi}{\partial Y^2}\right) + \frac{1}{\mathrm{Sc}}\left[n\mathrm{S} - \varepsilon_{\mathrm{c}}^n \mathrm{R}(\phi - \phi_0)\right] \tag{5}$$

where $n = 0$ or $n = 1$ respectively for flow outside and inside the porous matrix.

Dimensionless Cartesian coordinates X and Y, velocity components U and V, pressure P, temperature θ and ^{222}Rn activity concentration ϕ in the previous equations are defined as follows:

$$X = \frac{x}{H} \quad , \quad Y = \frac{y}{H} \quad , \quad U = \frac{uH}{\upsilon} \quad , \quad V = \frac{vH}{\upsilon} \quad , \quad P = \frac{pH^2}{\rho_0 \upsilon^2} \quad , \quad \theta = \frac{T - T_0}{\Delta T} \quad , \quad \phi = \frac{c_{\mathrm{a}} - c_0}{\Delta c} \tag{6}$$

while Darcy, Grashof, Prandtl, Schmidt numbers, decay-to-diffusion and emanation-to-diffusion ratios are given by

$$\mathrm{Da} = \frac{K}{H^2} \quad , \quad \mathrm{Gr} = \frac{g\,\beta\,\Delta T\,H^3}{\upsilon^2} \quad , \quad \mathrm{Pr} = \frac{\upsilon}{\alpha} \quad , \quad \mathrm{Sc} = \frac{\upsilon}{D_{\mathrm{o}}} \quad , \quad \mathrm{R} = \frac{\lambda H^2}{D_{\mathrm{o}}} \quad , \quad \mathrm{S} = \frac{\widetilde{G}H^2}{D_{\mathrm{o}}\Delta c} \tag{7}$$

Additional controlling parameters are the dimensionless activity level $\phi_0 = -c_0/\Delta c$ and bulk-to-fluid property ratios for kinematic viscosity $\Gamma = \widetilde{\upsilon}/\upsilon$, thermal diffusivity $\Lambda = \widetilde{\alpha}/\alpha$ and mass diffusivity $\Psi = \widetilde{D}/D_{\mathrm{o}}$. Details about the present model framework are presented in the first part of this paper.

2.2. Boundary conditions and dimensionless heat-mass transfer rates

The solution domain comprises atmospheric air and half of the phosphogypsum stack, as shown in Fig. 1. Both top horizontal ($Y = 2$) and left vertical ($X = 0$) boundaries are free surfaces for velocity components. The later is subjected to constant incoming temperature T_0 and ^{222}Rn activity concentration c_0 whereas developed profiles are assumed for the former. Symmetry is assumed about the right vertical boundary (X = 2A) and no-slip condition is applied to the horizontal impermeable ground ($Y = 0$). The ground temperature T_G beneath the stack is supposed higher than T_0 of the exposed ground. Moreover, instead of a stepwise function, an arbitrary steep exponential drop is considered between these two temperature levels. For such physical scenario, it is then suitable to define the following reference values

$$\Delta T = T_G - T_0 \qquad \text{and} \qquad \Delta c = \frac{\tilde{G}H^2}{D_o} \tag{8}$$

to scale temperature and ^{222}Rn activity concentration respectively in Eqs. (6). It is worth noting that, according to the last of Eqs. (7), the above definition for Δc implies S = 1.

Flux continuity is ensured by evaluating mean values of the physical properties at the two interfaces separating the open atmosphere and the air-saturated porous matrix. Wind effects and pressure fluctuations are not considered in this paper. Consistent with Fig. 1, the above adopted boundary conditions can be expressed in dimensionless form as

$$\text{at } X = 0: \quad \frac{\partial U}{\partial X} = \frac{\partial V}{\partial X} = P = 0 \qquad \theta = 0 \qquad \phi = 0 \tag{9}$$

$$\text{at } X = 2\text{A}: \quad U = \frac{\partial V}{\partial X} = 0 \qquad \frac{\partial \theta}{\partial X} = 0 \qquad \frac{\partial \phi}{\partial X} = 0 \tag{10}$$

$$\text{at } Y = 0: \quad U = V = 0 \qquad \theta = \begin{cases} e^{15(X-\text{A})}, & 0 \le X < \text{A} \\ 1, & \text{A} \le X \le 2\text{A} \end{cases} \qquad \frac{\partial \phi}{\partial Y} = 0 \tag{11}$$

$$\text{at } Y = 2: \quad \frac{\partial U}{\partial Y} = \frac{\partial V}{\partial Y} = P = 0 \qquad \frac{\partial \theta}{\partial Y} = 0 \qquad \frac{\partial \phi}{\partial Y} = 0 \tag{12}$$

As discussed in the first part of the paper, radiation exposure assessment and radiological protection design are based on ^{222}Rn exhalation rates. Taking into account both diffusive and convective fluxes (Andersen, 2000), normalized ^{222}Rn exhalation rates from the exposed top ($Y = 1$) and left ($X = 1$) surfaces of the phosphogypsum stack are assessed via average Sherwood number. Using $j_0 = \tilde{D}\Delta c / H$ as a normalizing scale, the corresponding expressions are

$$\text{Sh}_{\text{top}} = \frac{1}{\text{A}} \int_{\text{A}}^{2\text{A}} \left[\frac{\text{Sc}}{\Psi} V(\phi - \phi_0) - \frac{\partial \phi}{\partial Y} \right]_{Y=1} dX \qquad \text{and} \qquad \text{Sh}_{\text{left}} = -\int_0^1 \left[\frac{\text{Sc}}{\Psi} U(\phi - \phi_0) - \frac{\partial \phi}{\partial X} \right]_{X=1} dY \tag{13}$$

Similar rationale can be applied as far as dimensionless heat transfer rates are concerned. Normalizing conductive and convective heat fluxes by $\dot{q}_0'' = \tilde{k}\Delta T / H$, the average Nusselt number is assessed by

$$\text{Nu}_{\text{top}} = \frac{1}{\text{A}} \int_{\text{A}}^{2\text{A}} \left[\frac{\text{Pr}}{\Lambda} V\theta - \frac{\partial \theta}{\partial Y} \right]_{Y=1} dX \qquad \text{and} \qquad \text{Nu}_{\text{left}} = -\int_0^1 \left[\frac{\text{Pr}}{\Lambda} U\theta - \frac{\partial \theta}{\partial X} \right]_{X=1} dY \tag{14}$$

Leppinen and Rees (2003) presented a similar expression for the heat flux across a vertical plane within the core region of a porous matrix where the no-slip condition cannot be applied, analogous to what happens at the air-stack interfaces. Total average Sherwood and Nusselt numbers are simply calculated as

$$\text{Sh} = \text{Sh}_{\text{top}} + \text{Sh}_{\text{left}} \qquad \text{and} \qquad \text{Nu} = \text{Nu}_{\text{top}} + \text{Nu}_{\text{left}} \tag{15}$$

2.3. Representative values for the test case

Several physical factors influence the ^{222}Rn transport in porous media simultaneously. Although many of them can be grouped into dimensionless parameters, a systematic investigation of the effects of each controlling parameter is impractical. Typical values found in phosphogypsum problems were presented in the first part of the paper. Bearing in mind the physical scenario under analysis, the following representative values are adopted: A = 1.5, Da = 10^{-13}, Pr = 0.71, Sc = 1.25, $\Gamma = \Lambda = 1$, $\Psi = 0.1$, R = 0.5, $\varepsilon_c = 0.5$ and $\phi_0 = 0$ (for simplicity), apart from S = 1 as established by the above definition of the reference scale Δc.

Grashof number is the only variable parameter and it is allowed to span from 10^6 to 10^8 for the present test case. Accordingly, this preliminary study focuses on possible buoyant effects related to very small up to small temperature differences between the ground underneath the phosphogypsum stack base and the incoming atmospheric air. Neither external nor internal heat sources are considered in this investigation.

3. Numerical method

Numerical solutions are obtained by incorporating the new proposed expressions into an existing computational simulator that has been successfully used to solve heat and mass transfer problems in media partially or fully filled with porous material (Mohamad, 2003). Following a finite-volume method, governing equations are converted into an algebraic system after integration over each control volume in the solution domain. SIMPLER algorithm couples continuity and momentum equations and staggered grid arrangement is adopted in order to prevent pressure oscillations (Patankar, 1980). Algebraic equations are solved iteratively by the TDMA algorithm.

Under-relaxation factors are 0.7 for *U* and *V* velocity components and set to unity for the remaining primitive variables, except for the simulation corresponding to Gr = 10^8 in which case an under-relaxation factor of 0.9 is enough to prevent both θ and ϕ from diverging. Convergence criteria are based on local and global conservation of mass, momentum, energy and species (^{222}Rn activity) concentration within pre-established error tolerances. Details about the simulator are presented elsewhere (Mohamad and Bennacer, 2001; Bennacer *et al.*, 2001; Mohamad, 2003).

In order to ensure grid-size independent results, 8000 iterations were performed on the following mesh refinement sequence: 32 × 22, 62 × 42, 92 × 62, 122 × 82 and 152 × 102, using orthogonal structured regular grids. For this mesh sensitivity analysis Gr was set at 10^7. Table 1 presents total Nu and Sh as calculated according to Eqs. (13) through (15) as well as the absolute relative difference between the numerical values yielded from two consecutive mesh sizes (as distinguished by subscripts "next" and "prev"). It is seen that differences between numerical results from successive become rather small starting from the 122 × 82 mesh. Therefore, as a compromise between accuracy and computational effort, simulations presented in this paper were performed using the 152 × 102 regular grid.

Table 1. Total Nusselt and Sherwood numbers for mesh sensitivity analysis.

Mesh size	$Nu = Nu_{top} + Nu_{left}$	$\left\| 1 - \frac{Nu_{next}}{Nu_{prev}} \right\|$	$Sh = Sh_{top} + Sh_{left}$	$\left\| 1 - \frac{Sh_{next}}{Sh_{prev}} \right\|$
32 × 22	1.62		6.55	
62 × 42	2.14	32.1%	7.39	12.8%
92 × 62	1.94	9.3%	7.66	3.7%
122 × 82	2.00	3.1%	7.83	2.2%
152 × 102	2.02	1.0%	7.92	1.1%

4. Numerical results and discussion

Numerically simulated streamlines for Gr = 10^6, 10^7 and 10^8 are presented in Fig. 2. From the sequence, it can be observed that the flow field follows basically the same structure as Grashof number increases from Gr =10^6 to Gr = 10^8. Stream function values augment roughly by a factor of 2 as Gr increases by an order of magnitude. Small recirculation cells onset just above the top corner of the stack for Gr ≥ 10^7 whereas the ascending buoyancy-driven air flow is concentrated over the stack middle (around the symmetry line). Due to the relatively low Darcy number assumed, i.e. Da = 10^{-13}, incoming air virtually does not penetrate into the stack and it essentially flows around.

As a consequence, dimensionless temperature and concentration fields within the porous matrix are hardly affected by the outside air flow structure and strength, as respectively depicted in Figs. 3 and 4. Internal isoconcentration lines and isotherms are almost the same but an exception occurs from the isotherm corresponding to $\theta = 0.1$. Such isotherm is rather sensitive to the streamline pattern and, particularly for Gr = 10^6, it extends away from the stack top.

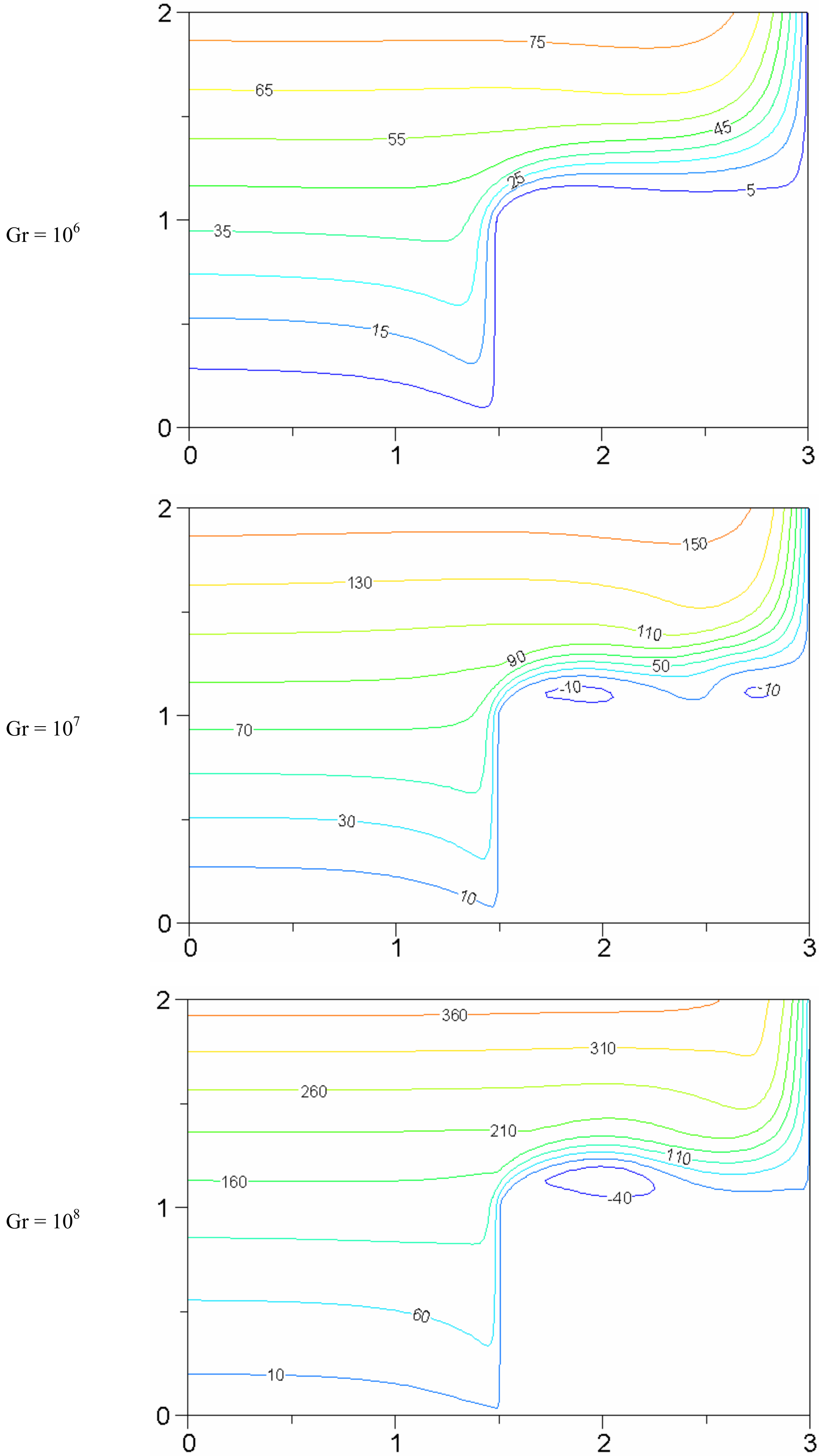

Figure 2. Numerically simulated streamlines for Gr = 10^6, 10^7 and 10^8.

Gr = 10^6

Gr = 10^7

Gr = 10^8

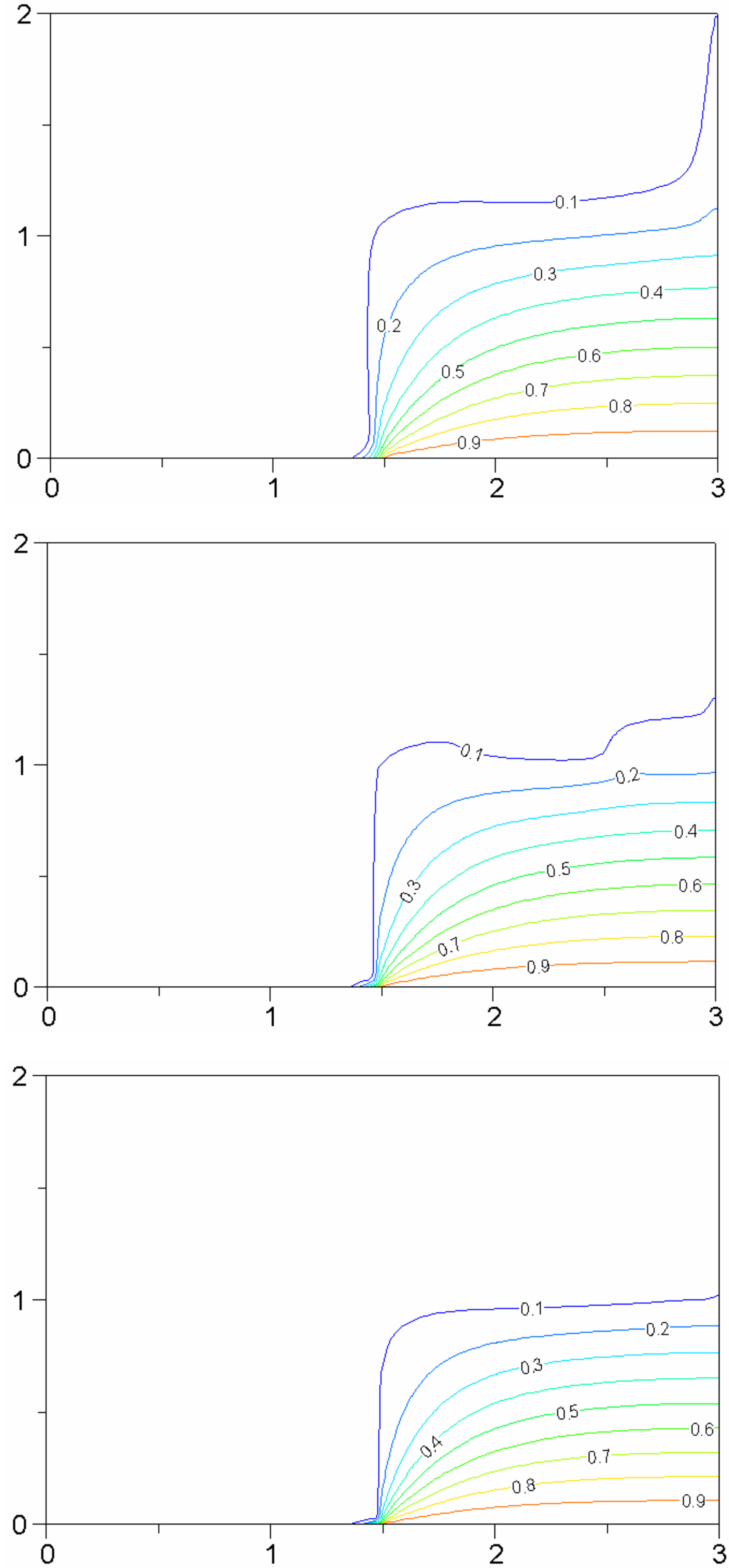

Figure 3. Numerically simulated isotherms for Gr = 10^6, 10^7 and 10^8.

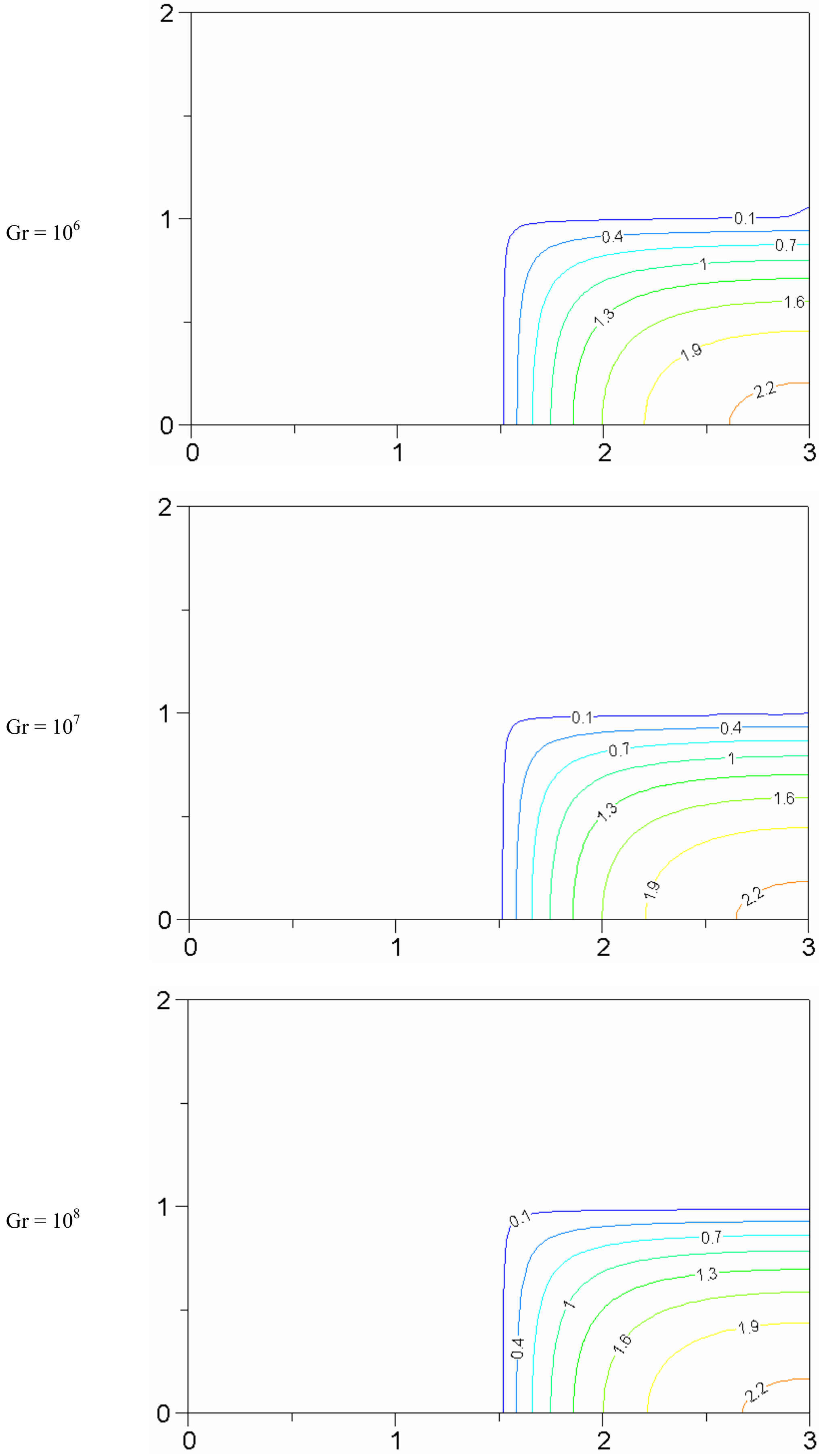

Figure 4. Numerically simulated isoconcentration lines for Gr = 10^6, 10^7 and 10^8.

Average Nusselt and Sherwood numbers at the stack top, at the stack left side and total (i.e. sum of top and side values), as calculated by Eqs. (13) to (15), are presented respectively in Figs. 5 and 6 as a function of Grashof number in the range $10^6 \leq Gr \leq 10^8$. Results for Nu show a slight increase with Gr, the contribution from the left side value being considerably higher than that from the top. This might stem from the fact that isotherms are more concentrated (hence, steeper temperature gradients) in the vicinity of the left vertical boundary than near the top horizontal boundary, as shown in Fig. 3

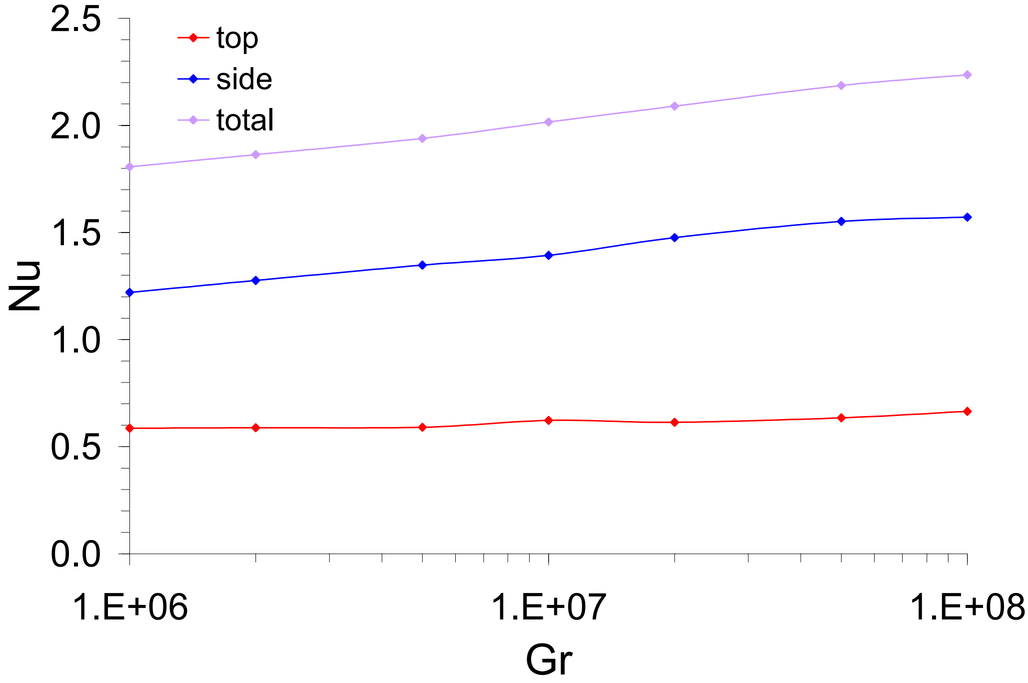

Figure 5. Average Nusselt number (at the stack top, at the stack left side and total) as a function of Grashof number.

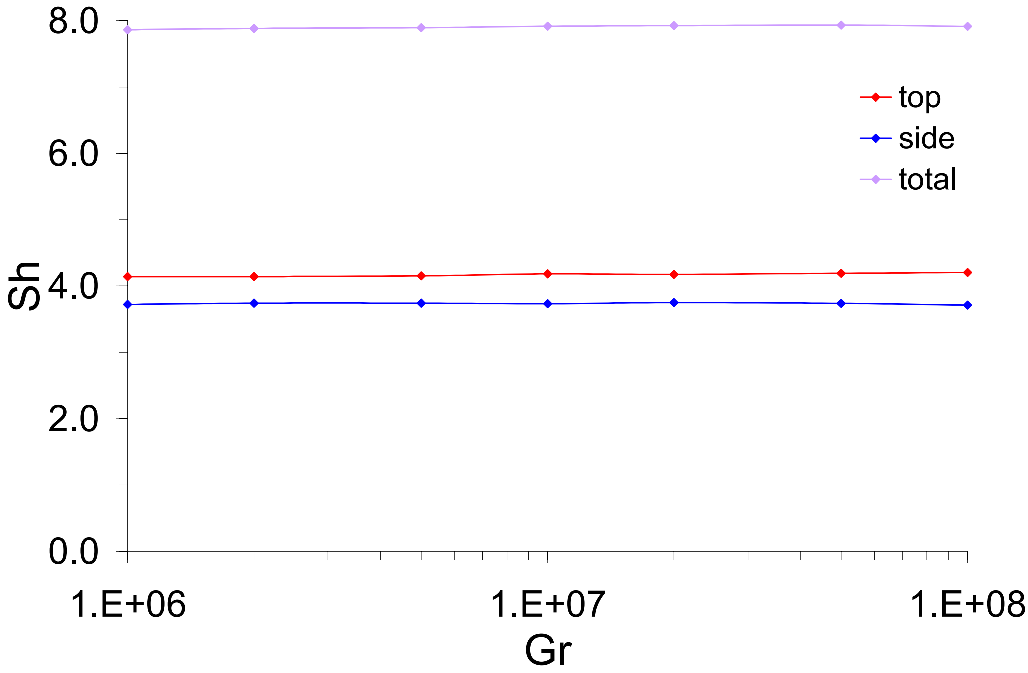

Figure 6. Average Sherwood number (at the stack top, at the stack left side and total) as a function of Grashof number.

On the other hand, isoconcentration lines seem to be rather equally spaced near the left vertical and top horizontal boundaries, as depicted in Fig. 4. As a consequence, ^{222}Rn activity concentration gradients seem to be uniform as well as of the same magnitude close to those two boundaries. This might be a reason for the average Sh at the stack top being just a bit higher than the left side counterpart. Nevertheless, both (and thus total Sh) are roughly insensitive to Gr

5. Concluding remarks

Radon exhalation from phosphogypsum-bearing materials involves numerous parameters and a comprehensive approach is likely to rely on numerical simulation. In this second part of the paper, the dimensionless model equations for ^{222}Rn transport in porous media outlined in the first part were solved numerically by adapting an existing simulator that has been successfully used to solve heat and mass transfer problems in porous media. As a test case, a rectangular shaped stack was considered. Among the assumptions, air flow was strictly buoyancy driven and the ground was impermeable to ^{222}Rn and at a higher temperature beneath the stack base. Dimensionless controlling parameters were set to representative values whereas Grashof number was allowed to vary within the range $10^6 \leq Gr \leq 10^8$.

Similar streamlines were numerically simulated for Gr = 10^6, 10^7 and 10^8 and both isotherms and isoconcentration lines remained almost unchanged within the porous matrix. As steeper temperature gradients occurred near the left vertical stack boundary, average Nusselt number near this boundary proved to be higher than the stack top counterpart. Conversely, because ^{222}Rn activity concentration gradients seemed to be uniform and of the same magnitude, average Sherwood number at the stack horizontal top and left vertical boundaries are approximately equal and quite insensitive to Grashof number. As an overall result, total average Sh proved to be insensitive to Gr.

For this particular low permeability phosphogypsum stack, results suggest that ^{222}Rn exhalation from inside the stack into the local atmosphere is strongly diffusive dominant and buoyant effects are of minor importance. It remains to be investigated whether the incoming fresh air is able to penetrate deeper into a loose packing (i.e. higher Darcy number) stack and enhances the interstitial convective ^{222}Rn transport within such porous matrix.

6. Acknowledgement

The first author is grateful to CAPES (Coordenação de Aperfeiçoamento de Pessoal de Nível Superior – Brazil) for their financial support (Process BEX 0624/03-9).

7. References

Andersen C.E., 2000, "Radon Transport Modelling: User's Guide to RnMod3d", Riso-R-1201(EN), Riso National Laboratory, Roskilde, Denmark.

Bennacer R., Mohamad A.A., Akrour D., 2001, "Transient natural convection in an enclosure with horizontal temperature and vertical solutal gradients", Int. J. Thermal Sciences, vol. 40, pp. 899-910.

Bertozzi D.A., Rabi J.A., Silva N.C., 2002, "Prediction of Rn-222 exhalation rates from phosphogypsum-based embankments. Part II: numerical simulation and results", Research Development Braz. J., vol. 4, n. 3, pp. 1199-1203.

Leppinen D.M., Rees D.A.S., 2003, "Convection in shallow rectangular cavities near the density maximum". IN: Ingham D.B. (ed.), "Current Issues on Heat and Mass Transfer in Porous Media – Proceedings of NATO Advanced Study Institute on Porous Media", Ovidius University Press, Neptun-Olimp, Romania.

Loureiro C.O., 1987, "Simulation of the steady-state transport of radon from soil into houses with basements under constant negative pressure", Ph.D. thesis, Environmental Health Sciences, University of Michigan, Ann Arbor, USA.

Mohamad A.A., 2003, "Heat transfer enhancements in heat exchangers fitted with porous media Part I: constant wall temperature", Int. J. Thermal Sciences, vol. 42, pp. 385-395.

Mohamad A.A., Bennacer R., 2001, "Natural convection in a confined saturated porous medium with horizontal temperature and vertical solutal gradients", Int. J. Thermal Sciences, vol. 40, pp. 82-93.

Nero A.V., 1988, "Radon and its decay products in indoor air: an overview". IN: Nazaroff W.W., Nero A.V. (eds.), "Radon and its Decay Products in Indoor Air", John Wiley & Sons, New York, USA.

Patankar S.V., 1980, "Numerical Heat Transfer and Fluid Flow", Hemisphere, New York, USA.

Rabi J.A., Mohamad A.A., 2004, "Radon-222 exhalation rates from phosphogypsum-bearing embankment subjected to constant temperature and fixed activity concentration", paper accepted for future publication in J. Porous Media.

Riley W.J., Robinson A.L., Gadgil A.J., Nazaroff W.W., 1999, Effects of variable wind speed and direction on radon transport from soil into buildings: model development and exploratory results, Atmosph. Environ., vol. 33, pp. 2157-2168.

Yu C., Loureiro C., Cheng J.J., Jones L.G., Wang Y.Y., Chia Y.P., Faillace E., 1993, "Data Collection Handbook to Support Modeling Impacts of Radioactive Materials in Soil", Environmental Assessment and Information Sciences Division, Argonne National Laboratory, Argonne, USA